Multiband left-handed metamaterials

Jiafu Wang,[1,a)] Shabo Qu,[1] Yiming Yang,[1] Hua Ma,[1] Xiang Wu,[1] and Zhuo Xu[2]
[1]*College of Science, Air Force Engineering University, Xi'an 710051, Shaanxi, People's Republic of China*
[2]*Electronic Materials Research Laboratory, Key Laboratory of the Ministry of Education, Xi'an Jiaotong University, Xi'an 710049, Shaanxi, People's Republic of China*

(Received 3 April 2009; accepted 12 June 2009; published online 7 July 2009)

A method of realizing multiband left-handed metamaterials (MB-LHMs) was presented. By alternatively stacking arrays of unit cells with different geometrical dimensions, the combined structures exhibit multiple LH passbands. As an example, a typical MB-LHM was designed, fabricated, and investigated numerically and experimentally. Both the simulation and experiment results show that the MB-LHM has three alternatively left- and right-handed passbands, of which two are LH ones. © *2009 American Institute of Physics*. [DOI: 10.1063/1.3170236]

Left-handed metamaterials (LHMs) with simultaneously negative μ and ε have been attracting great attentions since the work of Pendry *et al.*[1] and Smith *et al.*[2] in realizing the first LHM. Nowadays, the realization of broadband, low-loss LHMs is still the main topic of LHM research. A great variety of LHMs have been designed and fabricated. Generally speaking, presently existing LHMs fall roughly into three categories. The LHMs in the first category are based on metallic patterns. Both negative μ and ε are realized by the resonances of metallic patterns. LHMs composed of S-shaped,[3] Ω-shaped,[4] compound resonator unit cells,[5,6] as well as the so-called planar LHMs[7–10] fall into this category. LHMs in the second category are based on transmission lines.[11,12] Recently, many researchers are focusing on all-dielectric route to LHMs. Many all-dielectric LHM unit cells, such as the disklike unit cell,[13] were proposed. These unit cells are based on different resonance modes in all-dielectric unit cells. Under a certain resonance mode, the effective μ or ε is negative. By combing different all-dielectric unit cells, simultaneously negative μ and ε can be achieved.

The abovementioned LHMs have only one LH passband. In contrast, there are few studies on multiband (MB)-LHMs. Eleftheriades[14] proposed a generalized transmission-line-based LHM with two LH and two right-handed (RH) passbands. H. Lin *et al.*[15] presented arbitrary dual-band microstrip components based on composite right/LH transmission lines. Chen *et al.*[16] proposed a two-passband LHM based on S-shaped resonators. In this letter, a method of realizing MB-LHMs was proposed. By alternatively stacking arrays of LH unit cells with different geometrical dimensions, the combined structures can achieve multiple LH passbands. As an example, a MB-LHM composed of coplanar resonator unit cells was designed, fabricated and investigated to verify the design method.

Generally speaking, there is one particular LH band for one particular LH unit cell. Thus, N different unit cells can realize N different LH bands. If we combine N different LH unit cells in such a way that the size of the combined unit cell is far less than the wavelength, it is expected that the combined structure will exhibit multiple LH bands. Therefore, MB-LHMs can be realized by alternatively stacking arrays of different LH unit cells. As an example, a MB-LHM was designed by using the coplanar resonator unit cells.[5] The metallic patterns of the coplanar resonator unit cell are shown in Fig. 1. The gray parts denote metallic strips while the white parts denote the substrate. The square metallic ring with two splits serves as a magnetic resonator while the copper patterns in the center blank part of the square ring acts as an electric resonator. The electric resonator can realize negative ε while the magnetic resonator can realize negative μ. By carefully adjusting the geometrical dimensions of the two resonators, their negative response frequency ranges can be tuned to overlap. Simultaneously μ and ε can be realized in the overlapped frequency ranges.

Figure 2 illustrates the structure of the designed LHM with two LH passbands. There are two kinds of unit cells in all. They are of the same metallic patterns (shown in Fig. 1) but different geometrical dimensions. To fabricate the MB-LHM, the unit cell patterns are first etched on one side of the substrates. On each substrate, the unit cells are of the same geometrical dimension, so the substrates fall into two categories, as shown in Fig. 2. Dimensions of the unit cell on substrate 1 are: $a=3.3$ mm, $b_1=2.8$ mm, $b_2=1.7$ mm, $c=0.2$ mm, $d=0.2$ mm, $l=0.3$ mm, and $w=0.2$ mm. While dimensions of the unit cell on substrate 2 are: $a=3.3$ mm, $b_1=3$ mm, $b_2=1.9$ mm, $c=0.1$ mm, $d=0.2$ mm, $l=0.4$ mm, and $w=0.2$ mm. The two kinds of substrates are stacked alternatively side by side to form a bulk LHM, as shown in Fig. 2.

In order to verify the MB-LHM, numerical simulations were first carried out using the frequency domain solver of

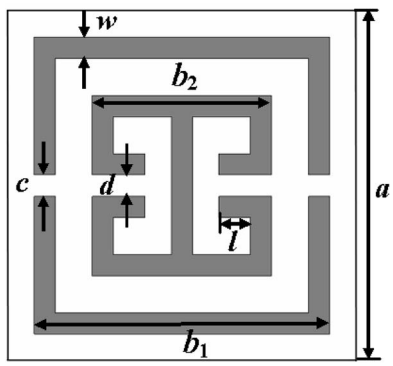

FIG. 1. The coplanar resonator unit cell.

a)Electronic mail: haomeijuan@126.com.

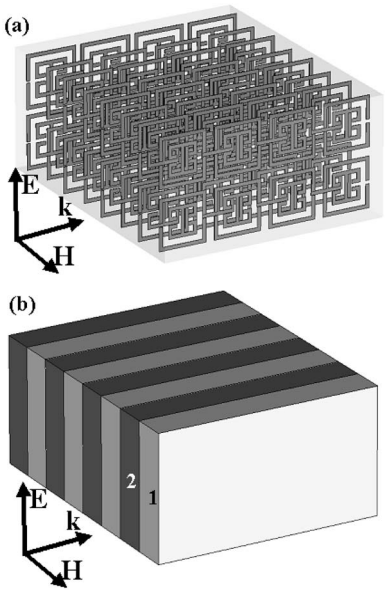

FIG. 2. Illustration of the proposed LHM with two LH passbands.

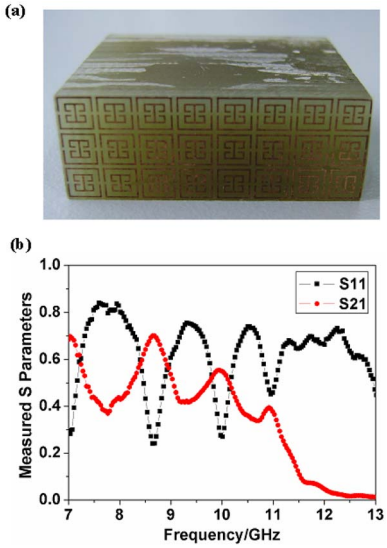

FIG. 4. (Color online) (a) Photograph of the fabricated sample and (b) the measured scattering parameters.

CST MICROWAVE STUDIO. In the simulations, the metal material we used is copper (conductivity $\sigma=5.8\times10^7$ S/m, thickness $t_1=0.017$ mm) and the substrate is FR4 (dielectric constant $\varepsilon_r=4.9$, thickness $t=3$ mm). By a standard algorithm,[17,18] effective constitutive parameters can be extracted from the scattering parameters. Figure 3 gives the simulated magnitudes of S_{11} and S_{21} parameters, as well as the retrieved real parts (solid curves) and imaginary parts (dashed curves) of effective permeability and permittivity. Figure 3(a) shows that there are three transmission peaks at 8.6, 10.0, and 11.0 GHz, respectively, which indicate three passbands. From Figs. 3(b) and 3(c), it can be found that in 8.6–9.7 and 11.0–11.5 GHz, real part of the effective permeability is negative, while real part of the effective permittivity is negative in 8.7–9.6 and 10.6–11.5 GHz. In the frequency ranges where both the real parts of effective permeability and permittivity are negative, LH passbands are expected. Thus, the two LH passbands are 8.7–9.6 and 11.0–11.5 GHz. The first and third passbands in Fig. 3(a) are LH, while the second one is RH.

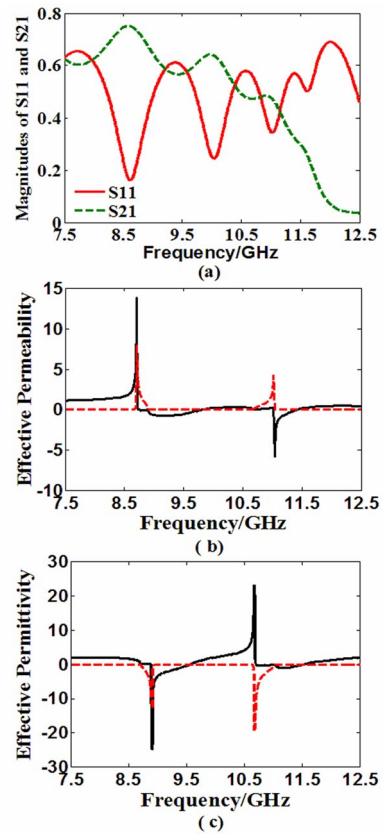

FIG. 3. (Color online) Simulated magnitudes of S_{11} and S_{21} parameters, as well as the real parts (solid curves) and imaginary parts (dashed curves) of effective parameters retrieved from simulated scattering parameters: (a) simulated magnitudes of S_{11} and S_{21}, (b) effective permeability, and (c) effective permittivity.

Note there is a RH passband between the two LH passbands. This is in clear contrast with the MB-LHM in Ref. 16 where there is a stopband between two LH passbands. The underlying reason for the difference lies in that the mechanisms of realizing LH passbands in the two cases are different. For the MB-LHM in Ref. 16, the permeability is negative only in the negative magnetic response frequency range, while the permittivity is negative over all the considered frequency range. Thus, outside the LH passbands, the permeability is positive while the permittivity is negative, so there is a stopband between two LH passbands. For the MB-LHM we presented in this letter, both the negative permeability and permittivity are realized by negative responses. The negative response bandwidths of magnetic and electric responses are usually not equal. As a result, outside the LH passbands, both the permeability and permittivity are positive. Therefore, there is usually a RH passband between two LH passbands.

The proposed MB-LHM was also fabricated and investigated experimentally. In practical fabrications, periodic arrays of copper (conductivity $\sigma=5.8\times10^7$ S/m, thickness $t_1=0.017$ mm) patterns were etched on the lossy FR4 substrate (dielectric constant $\varepsilon_r=4.9$, loss tangent tan $\delta=0.025$, thickness $t=3$ mm). Then the substrates were stacked alternatively and put together by adhesives. Photograph of the fabricated MB-LHM is shown in Fig. 4(a). The sample was put into a standard waveguide BJ100. Scattering parameters of the fabricated MB-LHM were measured by the Agilent

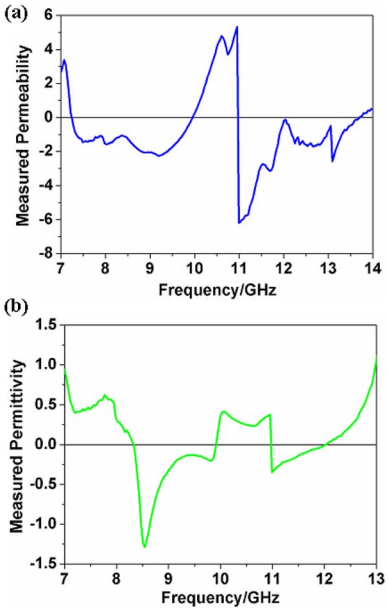

FIG. 5. (Color online) Real parts of (a) effective permeability and (b) effective permittivity retrieved from experimentally measured scattering parameters.

network analyzer HP8720ES. The measured S_{11} and S_{21} parameters are shown in Fig. 4(b). Comparing Figs. 3(a) and 4(b), we can find that the measured S_{11} and S_{21} parameters are almost the same as the simulated ones. There are also three transmission peaks around 8.6, 10.0, and 11.0 GHz, respectively. Note in both Figs. 3(a) and 4(b), the first transmission peak is the highest while the third one is the lowest. This can be explained by the loss brought about by the lossy FR4 substrates. As the frequency increases, the substrate loss becomes higher, resulting in the reduction of transmission. Note also the measured transmission is generally lower than the simulated one. This can be explained by the adhesives we used in the experiment, which introduce extra losses.

Figures 5(a) and 5(b) show, respectively, the real parts of effective permeability and permittivity retrieved from experimentally measured scattering parameters. The real part of effective permeability is negative in 7.2–9.9 and 11.0–13.6 GHz, while the real part of effective permittivity is negative in 8.3–9.9 and 11.0–12.0 GHz. Thus, the two LH passbands are 8.3–9.9 and 11.0–12.0 GHz. Between the two LH passbands, both the real parts of effective permeability and permittivity are positive, which means a RH passband. Note the measured two LH passbands are wider than the simulated ones. This difference is caused by the fabrication error as well as the adhesives we used.

In conclusion, we proposed a method of realizing MB-LHM by combing different LH unit cells. The number of LH passbands is dependent on the number of different LH unit cells in the combined LHM structures. As an example, we designed, fabricated and investigated a typical MB-LHM composed of coplanar resonator unit cells. Both the simulation and experiment results show that the LHM has two LH passbands, with a RH passband between them. To fabricate the MB-LHM, what we have to do is just to stack alternatively the substrates etched with different LH unit cells, so the MB-LHM can be conveniently fabricated for practical uses.

This work is supported in part by the National Natural Science Foundation of China under Grant Nos. 50632030 and 60871027 and in part by the 973 Project of Science and Technology Ministry of China under Grant No. 2009CB613306. The Natural Science Foundation of Shaanxi Province (Grant No. SJ08F01) also supports this work.

[1] J. B. Pendry, A. J. Holden, D. J. Robbins, and W. J. Stewart, IEEE Trans. Microwave Theory Tech. **47**, 2075 (1999).
[2] D. R. Smith, W. J. Padilla, D. C. Vier, S. C. Nemat-Nasser, and S. Schultz, Phys. Rev. Lett. **84**, 4184 (2000).
[3] H. Sh. Chen, L. X. Ran, J. T. Huangfu, X. M. Zhang, K. Sh. Chen, T. M. Grzegorczyk, and J. A. Kong, Appl. Phys. Lett. **86**, 151909 (2005).
[4] C. R. Simovski and S. L. He, Phys. Lett. A **311**, 254 (2003).
[5] J. F. Wang, Sh. B. Qu, Zh. Xu, J. Q. Zhang, Y. M. Yang, H. Ma, and Ch. Gu, Photonics Nanostruct. Fundam. Appl. **6**, 183 (2008).
[6] R. Liu, A. Degiron, J. J. Mock, and D. R. Smith, Appl. Phys. Lett. **90**, 263504 (2007).
[7] J. F. Zhou, L. Zhang, G. Tuttle, Th. Koschny, and C. M. Soukoulis, Phys. Rev. B **73**, 041101 (2006).
[8] K. B. Alici and E. Ozbay, Photonics Nanostruct. Fundam. Appl. **6**, 102 (2008).
[9] J. F. Zhou, Th. Koschny, L. Zhang, G. Tuttle, and C. M. Soukoulis, Appl. Phys. Lett. **88**, 221103 (2006).
[10] J. F. Wang, Sh. B. Qu, Zh. X, J. Q. Zhang, H. Ma, Y. M. Yang, and Ch. Gu, Photonics Nanostruct. Fundam. Appl. **7**, 108 (2009).
[11] E. Ozbay, K. Aydin, E. Cubukcu, and M. Bayindir, IEEE Trans. Antennas Propag. **51**, 2592 (2003).
[12] A. Lai, C. Caloz, and T. Itoh, IEEE Microw. Mag. **5**, 34 (2004).
[13] A. Ahmadi and H. Mosallaei, Phys. Rev. B **77**, 045104 (2008).
[14] G. V. Eleftheriades, IEEE Microw. Wirel. Compon. Lett. **17**, 415 (2007).
[15] I.-H. Lin, M. De Vincentis, C. Caloz, and T. Itoh, IEEE Trans. Microwave Theory Tech. **52**, 1142 (2004).
[16] H. Sh. Chen, L. X. Ran, J. T. Huangfu, X. M. Zhang, K. Sh. Chen, T. M. Grzegorczyk, and J. A. Kong, J. Appl. Phys. **96**, 5338 (2004).
[17] X. D. Chen, T. M. Grzegorczyk, B.-I. Wu, J. Pacheco, Jr., and J. A. Kong, Phys. Rev. E **70**, 016608 (2004).
[18] D. R. Smith, D. C. Vier, Th. Koschny, and C. M. Soukoulis, Phys. Rev. E **71**, 036617 (2005).